HHS Public Access

Author manuscript

Child Dev. Author manuscript; available in PMC 2017 September 01.

Published in final edited form as:

Child Dev. 2016 September ; 87(5): 1581–1600. doi:10.1111/cdev.12543.

The Cortical Development of Specialized Face Processing in Infancy

Maggie W. Guy, **Nicole Zieber**, and **John E. Richards**

Department of Psychology and Institute for Mind and Brain, University of South Carolina

Abstract

The aim of this study was to examine specialized face processing in 48 4.5- to 7.5-month-old infants by recording event-related potentials (ERPs) in response to faces and toys, and to determine the cortical sources of these signals using realistic, age-appropriate head models. All ERP components (i.e. N290, P400, Nc) showed greater amplitude during periods of attention than inattention. Amplitude was greater to faces than toys during attention at the N290, and greater to toys at the P400. Cortical source analysis revealed activity in occipital-temporal brain areas as the source of the N290, particularly the middle fusiform gyrus. The Nc and P400 were the result of activation in midline frontal and parietal, anterior temporal, and posterior temporal and occipital brain areas.

Introduction

Faces are processed in a manner distinct from other objects due to their social significance and ubiquity in our daily lives. This has been well documented in a large body of research with adult, children, and infant participants. Shortly after birth, infants demonstrate a looking preference for faces and face-like patterns (Goren, Sarty, & Wu, 1975; Johnson, Dziurawiec, Ellis, & Morton, 1991; Macchi Cassia, Turati, & Simion, 2004). Additionally, very young infants display a preference for their mother's face over a stranger's face (Bushnell, Sai, & Mullin, 1989; Pascalis, De Schonen, Morton, Deruelle, & Fabre-Grenet, 1995). These preferences are expected to become more specialized across the first years of life, resulting in the distinct patterns of neural activation seen in adults in response to faces compared with other classes of objects (e.g., Bentin, Allison, Puce, Perez, & McCarthy, 1996; Itier & Taylor, 2004; Kanwisher, McDermott, & Chun, 1997; Rossion, Hanseeuw, & Dricot, 2012; Sadeh, Podlipsky, Zhdanov, & Yovel, 2010). However, there has been less research examining the neural development of specialized face processing in infancy.

The aim of the current study was to expand current knowledge regarding face processing in infancy by recording event-related potentials (ERPs) in response to two classes of objects, faces and toys, and to determine the cortical sources of these neural signals. One goal was to explore developmental changes in the amplitude and latency of infant ERP components (i.e. N290, P400, Nc) in response to faces and toys at 4.5, 6, and 7.5 months of age. A second goal was to examine the effects of stimulus familiarity and salience on these ERP responses.

Contact Maggie W. Guy, Department of Psychology and Institute for Mind and Brain, Columbia, SC 29208, guymy@mailbox.sc.edu.

Third, we sought to accurately identify the neural generators of the ERP components by applying source localization techniques that utilized realistic, age appropriate head models.

Event-related potentials (ERPs) have been widely used in research examining the neural processing of faces across the lifespan. The ERPs are brief segments of electroencephalogram (EEG) recordings averaged together and time-locked with an event of interest, such as stimulus onset (Fabiani, Gratton, & Coles, 2000; Picton et al., 2000). The N170 is an ERP component commonly examined in face processing studies with adult participants. It is characterized by a negative peak that occurs approximately 170 ms after stimulus onset over occipito-temporal regions of the scalp. Greater N170 amplitudes are seen in response to human faces in comparison with objects such as houses, cars, and even animal faces (Bentin et al., 1996; Iidaka, Matsumoto, Haneda, Okada, & Sadato, 2006). The N170 is sensitive to the orientation of the face; it is enhanced for inverted faces relative to upright faces (Rossion et al., 2000), but not inverted versus upright objects or other species faces (Bentin et al., 1996). Furthermore, the N170 is sensitive to spatial attention (Eimer, 2000). It is greater in amplitude to attended than unattended peripherally presented faces, although this effect is not seen in examination of objects.

Evidence of specialized face processing has been found in infants in examination of two ERP components: the N290 and P400. The N290 shares some of the face-specific qualities associated with the adult N170 (Halit, de Haan, & Johnson, 2003). The N290 is seen in posterior electrodes and is characterized by a peak negative in amplitude occurring 290 to 350 ms after stimulus onset (de Haan, Johnson, & Halit, 2003; Halit et al., 2003). Like the N170, the infant N290 shows sensitivity to faces compared with other classes of visual stimuli. Greater amplitude N290 was found in response to faces than visual noise and in the right than left hemisphere when viewing faces in infants as young as 3 months of age (Halit, Csibra, Volein, & Johnson, 2004). The N290 has also shown sensitivity to specific characteristics of facial stimuli. Greater amplitude N290 was exhibited in response to familiar versus unfamiliar human and monkey faces in 9-month-olds (Scott, Shannon, & Nelson, 2006). The species-specific N170 inversion effect seen in adults has also been observed at the N290 in infants older than 6 months of age (de Haan, Pascalis, & Johnson, 2002; Halit et al., 2003). Overall, these findings suggest that as infant face processing becomes increasingly specialized, so does the N290 response.

The P400 has also been studied with respect to face processing in infant participants. It is a positive component that is maximal over occipital electrodes and that peaks between 390 and 450 ms after stimulus onset (de Haan et al., 2003). P400 latency is shorter to upright human faces compared with objects (de Haan & Nelson, 1999; McCleery, Akshoomoff, Dobkins, & Carver, 2009), visual noise (Halit et al., 2004), and inverted human faces (Halit et al., 2003). De Haan and Nelson (1999) hypothesized that shorter latencies in response to faces reflects rapid early encoding due to either low-level visual characteristics or a face-specific mechanism. Differences have also been reported in P400 amplitude based on stimulus type. In 6-month-old infants, P400 amplitude is more positive for upright than for inverted human and monkey faces (de Haan et al., 2002). The P400 may play a role in novelty detection; a greater amplitude response is sometimes seen to novel faces compared with familiar or standard faces (Key, Stone, & Williams, 2009; Scott et al., 2006).

The Nc component ("Negative Central", Courchesne, Ganz, & Norcia, 1981) is perhaps the most studied infant ERP component. The Nc is not a face-specific ERP component, but it is relevant to the examination of early face processing (de Haan et al., 2003). It is a negative component occurring between 350 and 750 ms after stimulus onset over frontal and central midline electrodes. The Nc is seen in response to objects and faces, but is typically higher in amplitude to salient or novel stimuli; it is thought to reflect attentional engagement and may be indicative of a looking preference (Courchesne et al., 1981; de Haan & Nelson, 1997, 1999; Guy, Reynolds, & Zhang, 2013; Reynolds et al., 2010; Richards, 2003; Webb et al., 2005). Richards and colleagues (Reynolds et al., 2010; Richards, 2003) investigated relations between infant heart rate (HR)-defined stages of attention and Nc amplitude and found greater amplitude during periods of attention than inattention. Evidence of the role of stimulus salience in the Nc response can be seen in studies examining the processing of meaningful stimuli, such as an infant's mother's face and favorite toy. Nelson and colleagues (de Haan & Nelson, 1997, 1999; Webb et al., 2005) found a greater amplitude Nc response to 6-month-olds' mother's faces than a dissimilar looking stranger's face and to their own toy than a novel toy (de Haan & Nelson, 1997, 1999; Webb et al., 2005).

The regions in the adult brain responsible for the specialized processing of faces have been studied extensively. Brain areas have been identified in adults through the use of functional magnetic resonance imaging (fMRI) that show greater activation in response to faces than to object and animal stimuli (e.g., Ishai, Ungerleider, Martin, Schouten, & Haxby, 1999; Kanwisher, Damian, & Harris, 1999; Kanwisher et al., 1997; Rossion et al., 2012; Sadeh et al., 2010). A particular area of the middle fusiform gyrus, labeled the fusiform face area (FFA), has consistently been shown to demonstrate greater activation to faces than other stimuli (Ishai et al., 1999; Kanwisher et al., 1997, 1999; Rossion et al., 2012). Activation of the FFA is thought to reflect the encoding of facial features and spatial relations among facial features (Kanwisher & Yovel, 2006). Several other brain areas have been identified that are involved in the processing of faces. These include the occipital face area (OFA), superior temporal sulcus (STS), and the anterior temporal face patch. The OFA, located on the lateral surface of the occipital lobe, is thought to represent feature selection of faces early in the processing stream (Pitcher, Walsh, & Duchaine, 2011). The STS shows greatest activation in response to dynamic aspects of face perception (Engell & Haxby, 2007; Ghazanfar, Chandrasekaran, & Logothetis, 2008). The anterior temporal face patch, which consists of a region in the anterior tip of the collateral sulcus, is thought to be more active during face recognition than object recognition (Nasr & Tootell, 2012).

Researchers have also used source localization of the N170 to investigate the brain areas involved in face processing in adult participants. A technique called "cortical source analysis" incorporates structural neuroimaging information with the electrical activity on the scalp to identify the neural generators in the cortex of ERP recorded on the scalp. Using this method a number of brain areas have been implicated in the generation of the N170. These include the fusiform gyrus (particularly the middle and posterior fusiform gyrus; Deffke et al., 2007; Rossion, Joyce, Cottrell, & Tarr, 2003; Shibata et al., 2002), the inferior temporal cortex (Shibata et al., 2002), the lateral occipital cortex (Rossion et al., 2003) and the STS (Itier & Taylor, 2004).

One study used cortical source analysis to examine the brain areas that may generate the N290 during face processing in infants (Johnson et al., 2005). Areas implicated included the right STS and surrounding temporal lobe areas, the lateral occipital cortex, and certain prefrontal regions. All identified brain regions were activated in response to faces at all ages tested, including 3-, 4-, and 12-month-olds. Areas within the right temporal lobe were most strongly associated with the N290. The primary goal of this work was to test whether regions involved in adult face processing were active in infancy. It did not pinpoint the specific neural generators responsible for the infant N290. Thus, some of the methods used in the study limit the conclusions that could be drawn regarding the source analysis of the N290.

Methods utilizing age-appropriate realistic head models with EEG recordings allow for the application of cortical source localization techniques to identify the neural generators (e.g., Richards, 2013). This may be especially important for infant participants, as great variation in size, structure, and topology of the brain even within a narrowly defined age (e.g., 6 months), requires individual or age-appropriate templates to perform accurate source localization with infants (Reynolds & Richards, 2009). Realistic head modeling requires the accurate co-registration of electrode positions on the scalp with MRI volumes from which the realistic head is determined (Darvas, Ermer, Mosher, & Leahy, 2006). Past studies of infant ERP source localization used less accurate head models. Johnson et al. (2005), for example, used individual head measurements but registered the electrode map to a 12-year-old participant's MRI. Others have used infant heads, such as the single MRI of one infant (Richards, 2005), the MRIs of a handful of 6-month-old infants (Reynolds et al., 2010), or less realistic, average head models (Hämäläinen et al., 2011; Ortiz-Mantilla et al., 2012). Thus, while Johnson and colleagues (2005) were able to conclude that several regions of the "social brain" are active in face processing in infancy, they acknowledged that the spatial resolution of the methods used was unclear. The optimal approach for electrical source analysis involves using realistic head models based upon individual participants.

The current study examined differences in the timing and morphology of the N290, P400, and Nc ERP components in response to face and toy stimuli in 4.5-, 6-, and 7.5-month-old infants. Heart rate was recorded to determine phases of attention and inattention throughout the experiment. We hypothesized that faces would elicit larger amplitude N290 responses and shorter latency P400 responses than toys. These components were expected to become more specialized for face processing with age, as evidenced by increased differentiation between responses to face and toy stimuli. Nc amplitude was predicted to be greater to the mother's face than stranger's face and to the familiar toy than the novel toy. Furthermore, the Nc was expected to be sensitive to the attentional state of the infant, as evidenced by a greater amplitude response during HR-defined periods of attention than inattention. It was unknown whether the N290 would be affected by attention because it may occur earlier in the processing stream than the impact of this factor, however results from the adult N170 literature showing greater amplitude to attended than unattended faces (e.g., Eimer, 2000) may relate to greater N290 amplitude during states of attention than inattention.

The second goal of the study was to determine the neural sources of the ERP components specific to face processing in infancy. We aimed to accurately identify neural regions

responsible for the components through the application of cortical source localization methods that included realistic head models based upon individual MRIs and age-appropriate infant templates. In the current study, we used volumetric current density reconstruction (CDR) and restricted our analyses to specific ROIs theoretically expected to be sensitive to faces. This results in more theoretically grounded source analysis than equivalent current dipole methods used in past work (e.g., Johnson et al., 2005; Hämäläinen et al., 2011; Ortiz-Mantilla et al., 2012, Richards, 2005). Current density was calculated at each source voxel within the head through the application of CDR, and source locations were restricted to a topography based on individual infant structural MRIs. For over half of the participants in this study, we had the infant's structural MRI and EEG data, thus the cortical source analysis was based on that infant's own MRI. Infants without their own MRI had a MRI selected for their head model that was close to the participant in age and head size.

Method

Participants

Forty-eight infants were recruited from Columbia, SC metropolitan area birth lists that were purchased from INFO USA (Omaha, NE). All infants were full term (at least 38 weeks gestation, birth weight at least 2,500 g) and healthy at birth with no known developmental anomalies. Participants were primarily Caucasian and of middle socioeconomic status. Participants included 14 4.5-month-old infants (mean age = 149.57 days; SD = 7.10; 9 males), 19 6-month-old infants (mean age = 184.67 days; SD = 7.80; 10 males), and 15 7.5-month-old infants (mean age = 230.00 days; SD = 15.12; 8 males). An additional 13 infants were tested, but excluded from the final sample because of fussiness (n = 5) or procedural error (n = 8). All infants participated with the informed, signed consent of their parents.

Stimuli

The stimuli consisted of pictures of faces and toys, and Sesame Street characters used as attractors, presented on variegated backgrounds. Figure 1 of the Supplemental Information shows sample stimuli. **Faces and toys**: The faces and toys were four images created from photographs taken after the participants arrived at the lab. Digital photographs were taken from a straight-on view of the mother's face and the infant's favorite toy. The background was removed from the images. The images of the participant's mother and toy were paired with photographs of the mother and toy from the previous participant. When presented on the monitor, the images measured approximately 17° visual angle. **Sesame Street Characters:** Moving videos of 15 Sesame Street characters were used as an attractor. The Sesame Street characters were taken from the movie, "Sesame Street's 25th Birthday: A Musical Celebration!" The video was edited to retain segments with only a single character from dancing scenes and contained just the character with dynamic movements. The characters were presented in a 2° × 3° area in the center of the screen. **Backgrounds**: Five static backgrounds containing only simple stimuli, such as water, sand, or grass, were presented on the entire monitor.

Apparatus and Procedure

Participants were seated on their mothers' laps, 55 cm away from a 29" LCD monitor (NEC Multisync XM29) in a darkened room. A video camera positioned above the monitor recorded the participants' faces. In an adjacent room, an experimenter viewed the infant on a TV monitor while controlling the stimulus presentations using an E-Prime experiment program. A Sesame Street character was presented in the center of the screen to attract the infant's fixation to the monitor. After the infant had fixated on the center of the screen, the experimenter began the trial by pressing a button. This initiated a sequence of brief image presentations and paired comparison (PC) trials. The brief stimulus presentations displayed a blank screen for a period of 100ms, followed by a 500 ms stimulus presentation, and a variable inter-trial interval of 500-1500 ms. The PC trials consisted of images of two faces (mother and stranger) or two toys (familiar toy and novel toy) presented side by side until 4 s of looking time was accumulated. The PC and brief trials were presented in a 10-trial block, including two brief presentations of the mother's face, stranger's face, familiar toy, and novel toy, one face PC, and one toy PC, presented in random order without replacement. A subset of the trials from a sample stimulus block is presented in Figure 1 of the Supplemental Information. An experimenter monitored fixations toward the screen. At the beginning of the experiment or if the infant looked away from the screen, a Sesame Street character was presented to draw fixation back toward the screen. A digital recording of the video was used to confirm offline that the infant was looking at the stimulus during the brief stimulus presentations and to measure visual preferences during the PC presentations. The purpose of the paired comparison procedure was to get preference measures for familiar and unfamiliar faces and toys (as well as to keep the infant interested). Trials continued as long as the infant was not fussy in order to obtain as many trials as possible.

Recording of ECG and Heart-Rate Defined Attention

The electrocardiogram (ECG) was recorded with two Ag-AgCl electrodes placed on the chest. These were digitized along with EEG with the EGI (Electrical Geodesics Incorporated, Eugene, OR) 128-channel EEG recording system (Johnson et al., 2001; Tucker, 1993). The ECG was analyzed offline to assess changes in HR to define periods of attention and inattention in a continuous presentation method (Mallin & Richards, 2013; Pempek et al., 2010; Reynolds et al., 2010). Periods of attention were defined as when the infant was looking toward the screen and showed a deceleration of HR below the prestimulus level (five beats with interbeat intervals (IBIs) > median prestimulus IBIs) and sustained lowered HR (IBIs > prestimulus median). The periods of inattention were defined as when the infant looked toward the screen and before the HR deceleration occurred, or continued looking toward the screen after the lowered HR returned to prestimulus levels, and until another significant HR deceleration occurred. If the infant looked away the attention phase was undefined, and then the sequence began again when the infant looked back toward the screen.

Recording and Segmenting of EEG

The EEG was recorded using the EGI 128-channel EEG recording system. Participants' were fitted with either a "geodesic sensor net" (GSN) or "hydrocel geodesic sensor net"

(HGSN; see the supplemental information for selection of GSN or HGSN nets). The size of the net was chosen based on the infant's head circumference. Net application took 5-10 minutes, during which a second experimenter entertained the infant with various toys. EEG was measured from 126 channels, from 124 channels in the electrode net and two Ag-AgCl electrodes that were used to measure electrooculogram (EOG). The EEG signal was referenced to the vertex, recorded with 20K amplification at a 250 Hz sampling rate with bandpass filters set from 0.1-100 Hz and 100 kΩ impedance. The vertex-referenced EEG was algebraically recomputed to an average reference. The EEG recordings were inspected for artifacts (?EEG > 100 μV), poor recordings, and eye movements using the ERPLab program and visual examination of EOG data. Individual channels or locations within trials were eliminated from the analyses if these occurred. If artifact was detected in more than ten channels within a trial, that trial was rejected from further analysis.

ERP Data Analysis

The EEG was filtered with a 0.5 Hz high-pass bandpass filter and the ERP trials were segmented from 50 ms before stimulus onset through 1 s following onset. The ERP data processing procedure was completed using the EEGLAB and ERPLAB toolboxes (Delorme & Makeig, 2004; Lopez-Calderon & Luck, 2014) within MATLAB (MATLAB R2014a, the Mathworks, Inc.). The EGI electrodes were combined into virtual "10-10" electrodes (see Supplemental Information, Table 1; electrodes were chosen from the GSN or HGSN column depending on the net used for a participant). Figure 1 shows the electrodes for the HGSN net along with the electrode clusters used to define the virtual 10-10 electrodes. The N290 was examined from 250-325 ms after stimulus onset at lateral posterior-inferior scalp areas (PO7-10, P7-10, and TP7-10) and the P400 from 350-750 ms after stimulus onset at medial posterior-inferior scalp areas (PO7-10, O1-2, I1-2, Oz, and Iz). The Nc was analyzed from 350-750 ms after stimulus onset at frontal and central midline virtual electrodes (Fz, FCz, and Cz). For analyses, virtual 10-10 electrodes used in examination of the N290 and P400 were grouped into Temporal Parietal, Lateral Parietal, Parietal Occipital, and Occipital Inion clusters, as shown in the ERP recordings in Figure 1.

Mixed-design ANOVAs were calculated to determine the effects of age, stimulus type, stimulus familiarity, HR-defined attention phase, electrode location, and hemisphere on N290, P400, and Nc peak amplitude and peak latency. The design for the study included age (3: 4.5 months, 6 months, 7.5 months) as a between subjects factor, and stimulus type (2: faces, toys), stimulus familiarity (2: familiar, novel), attention phase (2: attention, inattention), electrode location (2-3 based on analysis), and hemisphere (for N290 and P400, 2: left, right) as repeated measures factors. Three ANOVAs were calculated for each peak amplitude analysis: 1) examining effects of age, electrode location, and electrode hemisphere on grand average amplitude or latency; 2) examining main effects and interactions of stimulus type, stimulus familiarity, age, electrode location, and electrode hemisphere on component amplitude and latency; 3) examining main effects and interactions of stimulus type, attention phase, age, electrode location, and electrode hemisphere on component amplitude and latency. The factors of stimulus familiarity and attention were not analyzed as factors in the same ANOVAs because the interaction was not theoretically important to the current research questions. Latency effects were examined in a single

mixed-design ANOVA including age, stimulus type, electrode location, and electrode hemisphere. Latency effects were not examined for the Nc because they are not meaningful to the current study. Due to the unequal distribution of the number of trials in the cells of the factorial design, the ANOVAs were completed using the "Proc GLM" of SAS with a general linear models approach using nonorthogonal design (see Searle, 1987). The statistical tests used error terms derived from the related interval effect analyses and Scheffe-type methods to control for inflation of test wise error rate. Simple effects were examined through the calculation of least squares means. All significant tests are reported at $p < .05$.

Structural MRI and ROIs for Source Analysis

Structural (anatomical) MRIs were collected from 4.5-month-old (N = 7 of 14), 6-month-old (N = 9 of 19), and 7.5-month-old participants (N = 9 of 15). Participants in the current study that did not contribute their own MRI had an infant MRI chosen for them from the Neurodevelopmental MRI Database (Richards, Sanchez, Phillips-Meek, & Xie, 2015b; Richards & Xie, 2015). Recent research has indicated that source analysis using a similar individual MRI template provides more accurate results than analyses using average MRI templates (McCleery & Richards, 2012). More information on the selection of individual MRIs can be found in the Supplemental Information.

The MRIs were prepared for source analysis following the procedures previously detailed by Richards (2013; also see Supplemental Information). The MRIs were segmented into component materials including cerebral spinal fluid (CSF), white matter (WM), gray matter (GM), scalp, eyes, skull, and nasal cavity and a complete finite element method (FEM) model was computed for each MRI. The FEM model is a realistic head model that takes into consideration the geometry and conductivity of the materials within the head at the level of the voxel when determining the location of neural sources (Vatta, Meneghini, Esposito, Mininel, & Di Salle, 2010). An electrode placement map was constructed for the individual MRI by identifying fiducial electrode locations on the skull in the MRI volume, registering the fiducial locations on the skull to the same locations in an average electrode placement map from an age-appropriate average MRI template, and transforming the electrode placement map to fit into the AC-coordinate system for that participant (Richards, 2013; Richards, Boswell, Stevens, & Vendemia, 2015a; see Supplemental Information). An example of a segmented FEM wireframe, source volume, and electrode placement on an individual MRI can be seen in the Supplemental Information.

Anatomical regions of interest (ROIs) were identified in individual MRIs through the use of stereotaxic atlases created for each MRI (Filmore et al, submitted; Phillips et al., 2013). Lobar, LPBA40, and Hammers atlases were used to define several anatomical areas by identifying common designations from each of the atlases, and ROIs were mapped for each participant MRI. Eighteen ROIs were chosen for the source analysis based on previous research and theory regarding face-sensitive areas in the brain (e.g., Carlsson et al., 2008; Deffke et al., 2007; Itier & Taylor, 2004; Johnson et al., 2005). As this was the first detailed source analyses of these components in infancy, both areas where activation was expected based on previous literature (e.g., the fusiform gyrus) and several adjacent areas were included to ensure accurate detection of the source. The ROIs chosen included: the anterior

fusiform gyrus, middle fusiform gyrus, lateral inferior occipital gyrus, medial inferior occipital gyrus, lingual gyrus, inferior middle temporal gyrus, middle occipital lobe, parahippocampal gyrus, superior occipital gyrus, superior temporal gyrus, superior temporal sulcus, temporal pole, frontal pole, orbito-frontal gyrus, ventral anterior cingulate, dorsal anterior cingulate, posterior cingulate, and the superior parietal lobe. ROIs that showed a significant increase in activation in response to the experimental manipulation were included in the analysis. The subset of ROIs included in the source analysis of the N290 are identified in Figure 2 and mapped onto the 6-month-old average age appropriate template. The complete list of the anatomical areas making up the ROIs is presented in Supplemental Information Table 2.

Source Analysis with Realistic Head Models

Source analysis was completed with the individual realistic (FEM) head models to determine the cortical sources of the ERP electrical activity through the examination of current activity in the ROIs (Reynolds & Richards, 2009; Reynolds et al., 2010; Richards, 2013). Cortical sources were estimated with current density reconstruction (CDR; Darvas et al., 2001) using sLORETA (Pascual-Marqui, 2002; Pascual-Marqui, Michel, & Lehmann, 1994) as the constraint for the CDR. The source locations were defined by the segmented gray matter and the location of the eyes. The electrode locations, source locations, and head model were imported into EMSE's Data Analysis (Source Signal, Inc.) to produce estimates of the forward model, inverse model, and CDR.

All 126 electrodes used to measure EEG were included in the source analyses. Some channels were missing data either for the entire session or for individual trials. A linear interpolation was calculated to replace missing data within a trial using data from the five closest electrodes if fewer than ten electrodes were missing for an individual trial. If more than ten electrodes were missing within a trial, that trial was excluded from analyses. The ERP segments around the target onset were used in a 4-ms by 4-ms segment averaged over the appropriate experimental factors and conditions, and the entire ERP segment was used to estimate the CDR for each ERP slice. This resulted in a MRI volume representing the source volumes at each sampled ERP time. The MRI volume contained the current density for each voxel in the source. The current density was summed over each voxel of the ROI and divided by the total volume of the ROI, which resulted in an average CDR per mm^3 for each ROI. The CDR method has been used with realistic head models to successfully examine the sources of cortical activity within ROIs in infant and adult research (Hämäläinen et al., 2011; Ortiz-Mantilla et al., 2012, Richards, 2013). For the N290 analyses, we used the CDR data at the peak of the N290 ERP component. For the P400 and Nc analyses, we used the CDR data averaged from 400 to 600 ms following stimulus onset.

Results

ERP Analysis

Figure 1 shows the ERP responses at each of the virtual electrode clusters for the three ages tested. The P1 is evident as a small positive ERP component in the posterior-inferior electrodes peaking approximately 100 ms after stimulus onset. The N290 occurs in the

lateral posterior-inferior electrode sites (e.g., PO7-10, P7-10, TP7-10) about 300 ms post stimulus onset. In this figure, the N290 appears more peaked and increases in amplitude with age at the right electrode clusters. The P400 is seen from approximately 400-600 ms following stimulus onset at midline inferior-posterior electrodes. Finally, the Nc occurs from 350-750 ms after stimulus onset at frontal and central midline electrode locations.

On average each data collection session included 120 trials (SD = 33.63). Each participant contributed just over 80 total trials on average (M = 82.20, SD = 30.08, range 40-143) to the final data set, including approximately equal numbers of responses to faces (M = 40.27, SD = 15.91) and toys (M = 40.55, SD = 15.61). All participants contributed trials recorded during periods of attention and inattention, but overall more data was collected during inattention (M = 48.96 trials, SD = 21.49) than attention (M = 31.87 trials, SD = 16.42).

N290 Amplitude—A mixed ANOVA was carried out to examine the effects of age (3: 4.5-, 6-, 7.5-month-olds), electrode cluster (3: Parietal Occipital, Lateral Parietal, Temporal Parietal), and electrode hemisphere (2: left, right) on grand average N290 amplitude. Analysis of grand average N290 amplitude yielded no significant effects of age, electrode cluster, or electrode hemisphere. A second ANOVA included the factors of age, electrode cluster, electrode hemisphere, stimulus type (2: faces, toys), and stimulus familiarity (2: familiar, novel). Results yielded no significant effects of stimulus type and stimulus familiarity on N290 amplitude.

The effect of HR-defined attention phases on N290 responses were examined in a mixed ANOVA including, age, electrode location, electrode hemisphere, stimulus type (2: faces, toys), and attention phase (2: attention, inattention). There was a significant main effect of attention phase, $F(1, 45) = 7.10$, $p = .0107$. N290 amplitude was significantly greater during periods of attention, M = −5.03 μV, than inattention, M= −3.33 μV, $p < .0001$. Attention phase interacted with participant age, $F(2, 45) = 4.19$, $p = .0215$. At 4.5 months of age, participants responded with greater amplitude N290 during attention, M = −7.08 μV, than during inattention, M = −2.22 μV, $p < .0001$. Their N290 response during attention was significantly greater than that of 6- and 7.5-month-olds during attention (6: M = −3.82 μV, 7.5: M = −4.66 μV) and inattention (6: M = −3.39 μV, 7.5: M = −4.28 μV), all ps < .0001. Responses of 4.5-month-olds during inattention were significantly decreased in amplitude compared with older infants during attention or inattention, all ps < .0001. Six- and 7.5-month-old infants did not demonstrate significant differences in N290 amplitude across attention phases. However, 7.5-month-olds responded with greater N290 than 6-month-olds across periods of attention, $p = .0004$, and inattention, $p = .0001$. Figure 3 shows that the N290 differed in amplitude across attention phases and that this difference was greatest in 4.5-month-old participants.

The effect of attention on N290 responses also interacted with stimulus type and measures of scalp topography. There was an interaction of stimulus type and attention phase, $F(1, 45) = 6.92$, $p = .0116$. N290 amplitude in response to faces during attention, M = −6.89 μV, was significantly greater than in response to faces during inattention, M = −3.13 μV, and toys during attention, M = −3.17 μV, and inattention, M = −3.52 μV, all ps < .0001. There were no significant differences between responses to toys during attention and inattention.

Additionally, there was an interaction of attention phase, electrode cluster, and electrode hemisphere, $F(2, 90) = 6.57$, $p = .0022$. Amplitude of N290 responses was significantly greater during attention at right Lateral Parietal electrodes, M = −5.76 μV, than left Lateral Parietal electrodes, M = −4.51 μV, $p = .0002$. This effect was also seen at Parietal Occipital electrodes, N290 during attention at right electrodes, M = −5.74 μV, was significantly greater than left electrodes, M = −3.77 μV, $p < .0001$. Amplitude at Temporal Parietal electrodes did not differ across hemisphere during attention. N290 amplitude did not differ across electrode hemisphere during inattention for all electrode clusters, but was generally lower in amplitude than during attention.

N290 Latency—Mixed ANOVAs examined the effects of age (3: 4.5-, 6-, 7.5-month-olds), electrode cluster (3: Parietal Occipital, Lateral Parietal, Temporal Parietal), electrode hemisphere (2: left, right), and stimulus type (2: faces, toys) on N290 latency. Results revealed a main effect of electrode cluster, $F(2, 90) = 4.05$, $p = .0206$. As can be seen in Figure 1, latency to N290 peak was significantly longer at Temporal Parietal electrodes, M = 300.06 ms, than Parietal Occipital electrodes, M = 284.10 ms, $p = .0030$. There were no significant differences in latency at Lateral Parietal electrodes, M = 290.16 ms, and the other clusters. There was no effect of stimulus type (faces and toys) on N290 latency.

P400 Amplitude—Grand average P400 amplitude was examined in a mixed ANOVA including the factors, age (3: 4.5-, 6-, 7.5-month-olds), electrode cluster (2: Parietal Occipital, Occipital Inion), and electrode hemisphere (3: left, midline, right). Results included a main effect of electrode hemisphere, $F(2, 88) = 4.95$, $p = .0092$. Amplitude at left hemisphere electrode locations, M = 11.40 μV, was significantly greater than amplitude at right hemisphere electrode locations, M = 10.01 μV, $p < .0001$. There were no significant differences between these electrodes and amplitude at midline electrodes, M = 10.32 μV.

Responses to familiar and novel faces and toys were examined in a mixed ANOVA including age, electrode location, electrode hemisphere, stimulus type (2: faces, toys), and stimulus familiarity (2: familiar, novel). There was a main effect of stimulus type, $F(1, 44) = 5.98$, $p = .0186$. P400 amplitude was greater in response to toys, M = 14.47 μV, than faces, M = 11.80 μV. Figure 4 (right panel) presented P400 responses to faces and toys across attention phases and shows overall greater amplitude responses to toys than faces.

Amplitude of P400 responses during attention and inattention in response to faces and toys were examined in an ANOVA including the factors of age, electrode location, electrode hemisphere, stimulus type (2: faces, toys), and HR-defined attention phase (2: attention, inattention). There was a main effect of attention phase on P400 amplitude, $F(1, 43) = 8.00$, $p = .0071$. Figure 4 (left panel) shows ERP responses during attention and inattention summed over the two electrode clusters and across age. P400 amplitude was significantly greater during attention, M = 15.95 μV, than inattention, M = 11.97 μV. There was a marginally significant interaction of stimulus type, attention phase, and age, $F(2, 43) = 3.18$, $p = .0513$. Figure 4 (right panel) shows the ERP response separately for the three ages in response to faces and toys during attention and inattention. It can be seen in that P400 amplitude to toys during attention was greater than during inattention at all three ages. Amplitude of response to faces did not differ across attention and inattention for 6- and 7.5-

month-olds, but 4.5-month-olds showed a greater P400 response to faces during attention than inattention.

P400 Latency—P400 grand average latency was examined with a mixed-design ANOVA including the factors of age (3: 4.5-, 6-, 7.5-month-olds), electrode cluster (2: Parietal Occipital, Occipital Inion), electrode hemisphere (3: left, midline, right), and stimulus type (2: faces, toys). There was a main effect of electrode cluster, $F(1, 44) = 5.52$, $p = .0233$. Latency to P400 peak amplitude was shorter at Occipital Inion electrodes, M = 512.34 ms, than Parietal Occipital electrodes, M = 533.66 ms (see Figure 1). Results also included a significant interaction of age and electrode cluster, $F(2, 44) = 3.57$, $p = .0366$. Latency to P400 peak was significantly longer in 4.5-month-olds at Parietal Occipital clusters, M = 551.86 ms, than at other electrode locations and ages, all ps < .05. There were no significant effects of P400 latency to faces and toys.

Nc Amplitude—Grand average Nc amplitude was examined in a mixed-design ANOVA including the factors, age (3: 4.5-, 6-, 7.5-month-olds) and electrode cluster (3: FrontalZ, FrontalCentralZ, CentralZ), which yielded no significant effects. A mixed ANOVA was calculated to examine the factors of age, electrode cluster, stimulus type (2: faces, toys), and stimulus familiarity (2: familiar, novel). There were no significant effects of stimulus type or stimulus familiarity on Nc amplitude.

The effects of attention on Nc amplitude were examined in an ANOVA with the factors, age, electrode cluster, stimulus type, and attention phase (2: attention, inattention). There was a significant main effect of attention phase on Nc amplitude, $F(1, 43) = 7.76$, $p = .0079$. Figure 5 shows the ERP plots (left panel) from the mean midline virtual electrodes as a function of time and separately for attention and inattention. The Nc amplitude was greater during attention, M = −10.49 μV, than inattention, M = −7.43 μV, $p < .0001$. This is also seen in the topographical scalp potential maps in Figure 5 (right panel). It can be seen that the Nc difference in attention was scattered across both FrontocentralZ and CentralZ sites.

Cortical Source Analysis

Figure 2 presents the ROIs that demonstrated significant increases in activation in response to our experimental manipulations. These consisted of lateral and medial locations along the temporal lobe, including the middle fusiform gyrus, anterior fusiform gyrus, parahippocampal gyrus, lingual gyrus, and temporal pole. Figure 6 shows results from three ROIs at the latency of the N290 response. The current density amplitude increased with age across ROIs and different patterns of activation in response to faces and toys emerged with age. We calculated the linear and quadratic polynomial trends in the ROI activation over time to quantify these patterns. The youngest age had predominantly linear slopes of activation in response to faces and toys. At 6 months of age, there were both linear slopes, and an emerging negative quadratic trend. At 7.5 months of age, the response to toys was primarily linear in nature, whereas the response to the faces showed a strong negative quadratic trend. This is reflected in the peaked activation to faces in Figure 6 in the middle fusiform gyrus and the anterior fusiform gyrus for 7.5-month-olds. The linear trend to both faces and toys likely reflects the emerging P400 and Nc activity occurring after the N290

latency, whereas the quadratic trend to faces in the older participants reflects the cortical source of the N290 deflection in the ERP.

CDR amplitude during the time window of the N290—Cortical source analyses for the N290 were separated into anterior (anterior fusiform gyrus, parahippocampal gyrus, temporal pole) and posterior (middle fusiform gyrus, lingual gyrus, lateral inferior occipital lobe) ROIs. Mixed ANOVAs examining CDR with factors including age, ROI, hemisphere, and face and toy stimuli revealed significant main effects of age for both analyses: anterior ROIs, $F(2, 45) = 3.21$, $p = .0497$, and posterior ROIs, $F(2, 45) = 4.27$, $p = .0201$. Figure 7 shows the CDR for all ROIs that were significantly affected by the experimental variables. This figure shows an increase in CDR amplitude from 4.5 to 6 months, and from 6 to 7.5 months (all p values < .0001). There were also significant main effects of ROI for both analyses: anterior ROIs, $F(2, 90) = 5.30$, $p = .0067$, and posterior ROIs, $F(2, 90) = 46.61$, $p < .0001$. In anterior ROIs, there was greater current density amplitude in the anterior fusiform gyrus and parahippocampal gyrus than the temporal pole (Figure 7, left figures), both ps < .0001. In posterior ROIs, current density amplitude was greater in the middle fusiform gyrus than the lingual gyrus or the lateral inferior occipital gyrus (Figure 7, right figures), both ps < .0001, and in the lingual gyrus than the lateral inferior occipital gyrus, $p < .0001$. There was a significant interaction of age and ROI in the anterior ROIs, $F(4, 90) = 3.28$, $p = .0146$. Both 6- and 7.5-month-olds demonstrated the pattern of activation described above (greater CDR amplitude in the anterior fusiform and parahippocampal gyri than the temporal pole), but 4.5-month-olds demonstrated equal activation across the three ROIs. Note in Figure 7 the peaked nature of the response to faces in the 7.5-month-olds in the middle fusiform gyrus, anterior fusiform gyrus, and parahippocampal gyrus, but not in the temporal lobe (cf. Figure 6, negative quadratic polynomial trend).

CDR amplitude during the time window of the P400 and Nc—P400 and Nc sources were examined using mean activation from 400-600 ms after stimulus onset. This time window was selected based upon visual inspection of ERP and cortical activation and captured the peaks of both components. Latency to the peak of the P400 ERP component fell well into the Nc time window and an earlier peak (around 400 ms) was not seen in plots of activation in our source analysis results. Therefore we could not separate these components in the current source analysis. During the time window of the P400 and Nc ERP components, increased CDR amplitude was seen in the following ROIs, which were divided into three separate analyses as presented in Figure 8: midline frontal and parietal ROIs including the orbitofrontal gyrus, posterior cingulate, and ventral anterior cingulate; anterior temporal ROIs including the temporal pole, parahippocampal gyrus, and anterior fusiform gyrus; posterior temporal and occipital ROIs including the middle fusiform gyrus, lingual gyrus, middle inferior temporal gyrus, and medial inferior occipital gyrus.

Mixed ANOVAs examining factors including age, ROI, hemisphere, and CDR to face and toy stimuli revealed a main effect of ROI in posterior temporal and occipital ROIs, $F(3, 132) = 32.37$, $p < .0001$, and anterior temporal ROIs, $F(2, 88) = 18.96$, $p < .0001$. At posterior temporal and occipital ROIs current density amplitude was greater in the middle fusiform gyrus than the lingual gyrus, medial inferior occipital gyrus, or middle inferior temporal

gyrus, all p's < .0001, amplitude was also greater in the lingual gyrus than the medial inferior occipital gyrus or the middle inferior temporal gyrus, both $p < .0001$. At anterior temporal ROIs current density amplitude was greater in the anterior fusiform gyrus and parahippocampal gyrus than the temporal pole, both $p < .0001$. There were no significant effects in examination of the midline frontal and parietal ROIs.

An additional series of ANOVAs examined current density amplitude in response to faces and toys during HR-defined phases of attention and the results are shown in Figure 8. The main effect of ROI was replicated at posterior temporal and occipital ROIs, $F(3, 132) = 28.26$, $p < .0001$ (Figure 8 right), and anterior temporal ROIs, $F(2, 88) = 11.59$, $p < .0001$ (Figure 8 bottom left). Additionally, at the posterior temporal and occipital ROIs there was an interaction of ROI, stimulus type, and hemisphere, $F(3, 132) = 4.72$, $p = .0037$ and an interaction of ROI, stimulus type, hemisphere and age, $F(6, 132) = 3.82$, $p = .0015$. These interactions reflect generally greater amplitude in posterior temporal and occipital ROIs within the right hemisphere in response to faces during attention compared with toys during attention. This trend was only significant in 4.5-month-olds. CDR amplitude was significantly greater in the right than left middle inferior temporal gyrus in 4.5-month-olds, $p < .0001$. Additionally, 4.5-month-olds demonstrated significantly greater amplitude responses to faces during attention than toys during attention in right middle fusiform gyrus, $p = .0378$, and right middle inferior temporal gyrus, $p = .0006$. Furthermore, in the analyses of faces and toys during attention, there was a main effect of ROI at frontal and parietal ROIs, $F(2, 88) = 4.43$, $p = .0146$ (Figure 8 top left). Current density amplitude was greater in the orbitofrontal gyrus and the ventral anterior cingulate than the posterior cingulate, both $p < .0001$.

Discussion

We sought to enhance understanding of the development of specialized face processing in infancy. One goal was to explore changes in the timing and morphology of ERP components in response to face and toy stimuli in 4.5-, 6-, and 7.5-month-olds. The N290 amplitude was greater in response to faces than toys, but only during HR-defined periods of attention and primarily in younger infants. The amplitude of the P400 was greater to toys than faces, but peak latency did not differ to faces and toys. The amplitude of Nc was greater during attention than inattention. Our second goal was to examine the neural sources of these ERP components. Source analysis of the N290 component revealed significant levels of activation in the middle fusiform gyrus, anterior fusiform gyrus, parrahippocampal gyrus, and temporal pole. Examination of current density amplitude for the P400 and Nc ERP components revealed significant increases in activation in the orbitofrontal gyrus, posterior cingulate, ventral anterior cingulate, anterior fusiform gyrus, parahippocampal gyrus, temporal pole, middle fusiform gyrus, lingual gyrus, medial inferior occipital gyrus, and the inferior middle temporal gyrus.

We were particularly interested in the N290 and its role as the possible precursor to the adult N170. The results indicated that the N290 is a face-sensitive ERP component, but that attention is important to its responsiveness as specialized face processing develops in young infants. The 4.5-month-olds showed larger responses to faces and toys during attention,

whereas smaller differences were seen in 6- and 7.5-month-olds. This may reflect the increased automaticity of face detection at the older ages. Kouider and colleagues (2013) found enhanced N290 amplitude in response to faces compared with control visual noise stimuli in 12- and 15-month-old infants, but not 5-month-olds. Attention may play a smaller role in N290 responses with age, as the N290 begins to reflect a more automatic process of face detection, evidenced by converging N290 amplitudes during attention and inattention and greater amplitude responses to faces across all levels of attention.

The N290 ERP component was examined at parietal occipital, lateral parietal, and temporal parietal electrode clusters. Past research has primarily focused on only a subset of these areas, resulting in great variation in N290 ERP results in the literature. For instance, solely medial electrode sites have been utilized in one collection of studies (e.g., Kouider et al., 2013; Peykarjou, Pauen, & Hoehl, 2014; Scott & Monesson, 2010), lateral sites in another (e.g., Key & Stone, 2012; Macchi Cassia, Kuefner, Westerlund, & Nelson, 2006; McCleery et al., 2009), and an assortment of medial and lateral sites in a third group (e.g., de Haan et al., 2002; Halit et al., 2003, 2004; Lepännen, Moulson, Vogel-Farley, & Nelson, 2007). There was an early negativity following the P1 ERP component seen at medial electrode locations, which appeared much earlier than the N290 (cf. early negativity in Kouider et al., 2013). This ERP component is not likely generated by the same source as the N290, which is generated by current sources located anterior to the occipital scalp region and directed down and toward parietal occipital electrodes. Therefore, optimal N290 measurement should utilize lateral parietal electrodes (e.g., P7, P8, P9, P10) with electrode coverage extending below the traditional 10-20 electrode layout. These recommendations are congruent with the source of the N290 from within the fusiform gyrus as dipole current is expected to be more lateral than central.

The second purpose of the current study was to examine the neural sources of face-sensitive ERP components in infancy. Similar to the results of Johnson and colleagues' (2005) investigation of N290 sources, the areas of significant activation during the N290 latency period were in the temporal lobe. Analysis of cortical sources of the N290 component revealed significant levels of activation in the middle fusiform gyrus, anterior fusiform gyrus, parrahippocampal gyrus, and temporal pole. Of particular interest was the peaked current density response occurring in the middle fusiform gyrus, anterior fusiform gyrus, and parahippocampal gyrus (Figure 7). The peaked activity was found in 6- and 7.5-month-olds in response to the face stimuli and coincided with the N290 deflection in the ERP (Figure 1). The cortical sources of the N290 in response to faces were concentrated in the middle fusiform gyrus and spread across the other areas to a lesser degree. Areas within the fusiform gyrus have been implicated in face processing from studies of adult N170 source analysis (Deffke et al., 2007; Rossion et al., 2003; Shibata et al., 2002) and as the site of the FFA in adults (Kanwisher et al., 1997). Although the sources of the N290 are more widespread than those implicated in source analysis of the N170, the increasing differentiation of responses in the middle fusiform gyrus seen in our study over age may reflect the development of specialized face processing in this brain area. From the current study, we cannot determine if the N290 in infancy is the direct precursor to the N170 in adults. This is due to the difficulty of relating infant to adult ERP components, differences in the latency of the N290 and N170, and in functional relations between these components and

psychological processes that may differ in infant and adult participants. However, similarities in scalp locations and negative polarity are likely due to the generators of the N290 and the N170 being from comparable areas in the fusiform gyrus. It is possible that with age N290 amplitude become more strongly associated with fusiform gyrus activation. As indicated in previous studies (Kouider et al., 2013), face processing becomes more automatic with age and activation of these areas should become increasingly differentiated to faces. Future research could examine the stability of the fusiform gyrus as the generator of the N290 across the first years of life to associate it more directly with the N170.

We also explored the P400 and Nc ERP components. The P400 latency did not differentiate face and toy stimuli, differing from previously reported results (e.g., de Haan & Nelson, 1999; McCleery et al., 2009). De Haan and Nelson (1999) hypothesized that shorter P400 latency to faces than toys represented rapid encoding of faces compared with objects due to low-level characteristics of faces or a specific face processing mechanism. Our results did not support this conclusion and may indicate that the P400 is more sensitive to objects than faces, as greater amplitude was seen in response to toys than faces. It has been proposed that P400 amplitude may be an index of novelty detection (Key et al., 2009; Scott et al., 2006). The current results are difficult to interpret from this perspective. If novelty detection was facilitated in toys compared with faces, this pattern would be expected in the results of the Nc analysis as well.

The results of the Nc amplitude analysis were expected to replicate previous findings reflecting sensitivity to attentional states of the infants (Reynolds et al., 2010; Richards, 2003) and the salience of the mother's face and familiar toy (de Haan & Nelson, 1997, 1999). The Nc was sensitive to HR-defined periods of attention, as amplitude was greater during attention than inattention. Unlike results seen in the studies conducted by de Haan and Nelson (1997, 1999), the Nc amplitude did not differ to the mother's face and to a stranger's face. It is possible that this was due to patterns of similarity and dissimilarity in the faces used in this study and in de Haan and Nelson's. De Haan and Nelson (1997) only saw significant differences in Nc responses to the mother's face and stranger's face when they were rated as dissimilar in appearance. Differences in response to the mother's face and similar looking stranger's face, were not seen in the Nc, but were seen in an undefined mid-latency positive component over temporal electrodes. The novel face utilized in the current study was of the mother of the previous infant to participate in the study, and we did not control for the similarity of the participants across infants.

Current density amplitude was examined simultaneously for the P400 and Nc ERP components. Activation was found across a wide area of the anterior temporal lobe and prefrontal cortex during this time period, with greater activation to faces than toys during attention. Studies examining adult fMRI responses to faces and other objects have found increased activation to faces in similar areas, including the fusiform gyrus (Ishai et al., 1999; Kanwisher et al., 1997, 1999; Rossion et al., 2012), superior temporal gyrus and sulcus (Engell & Haxby, 2007; Ghazanfar et al., 2008), and the anterior temporal cortex (Nasr & Tootell, 2012; Shibata et al, 2002). These results identify several areas of the brain involved in the processing of faces beyond the N290 latency.

Distinct peaks for the P400 and the Nc sources were not identified in the source analysis. We visually inspected the results of our source analysis for peaks in activation around 400-500 ms, but did not find separate peaks in that period (Figure 8). In fact, the ERP averages in the posterior electrodes seem to show a distinct peak at about 400 ms, but then continue with the positive potential through the time period of the Nc (Figure 1; cf. Figures 4, 5). Thus we were not able to identify the specific neural sources of the P400 component. We believe that the pattern of the source analysis and ERP in this time range implies that there is early P400 activity that is independent of the neural activation for the Nc, but that much of the activity in this region is merely the positive expression of the dipole sources generating the Nc. The P400 peak analysis may be confounded with the Nc because of this. Long P400 latencies have been reported in previous studies (e.g., Halit, Csibra, Volein, & Johnson, 2004; Halit, de Haan, & Johnson, 2003; Macchi Cassia, Kuefner, Westerlund, & Nelson, 2006). In our study P400 latencies were greater than 500 ms (512 to 551 ms), and were longest in the youngest infants. Halit, de Haan, and Johnson (2003) reported a significant reduction in P400 latency from 3- to 12-month-olds. It is possible that the P400 activity is more confounded with the Nc component at the earliest ages used in our study, and then becomes increasingly distinct from the Nc with age. Source analysis conducted with older infants (i.e. 9- or 12-month-olds) may be able to more effectively separate the P400 response from the Nc to investigate unique neural sources.

The results of this study found differential processing of faces and toys at all ERP components examined and revealed developmental changes in the ERP components and their neural sources. Attention phases played a large role in these differences. Across all ERP analyses, HR-defined periods of attention were associated with greater amplitude responses. This study was the first to use realistic head models to examine the neural sources of face processing. Current density reconstruction was conducted using realistic, FEM models of individual infants' heads to determine regions of the brain that showed greater activation during the time periods of the ERP components of interest in response to faces and toys. N290 and P400 activity were both highly correlated with activation in the fusiform gyrus. The P400 and Nc components were also associated with activation in the orbitofrontal gyrus and ventral anterior cingulate. The current density amplitude in response to faces showed an increasingly quadratic pattern of activation with increased age, while toys did not. This emerging change in activation reflects emerging specialization of face processing in infancy. This study provides a window into the early development of specialized cortical activity during face processing and highlights the need for further research to examine these effects at additional ages in more diverse populations.

Supplementary Material

Refer to Web version on PubMed Central for supplementary material.

Acknowledgments

This research was supported by R37 HD18942 to JER.

References

Bentin S, Allison T, Puce A, Perez E, McCarthy G. Electrophysiological studies of face perception in humans. Journal of Cognitive Neuroscience. 1996; 8:551–565. [PubMed: 20740065]

Bushnell IWR, Sai F, Mullin JT. Neonatal recognition of the mother's face. British Journal of Developmental Psychology. 1989; 7:3–15.

Carlsson J, Lagercrantz H, Olson L, Printz G, Bartocci M. Activation of the right fronto-temporal cortex during maternal facial recognition in young infants. Acta Pædiatrica. 2008; 97:1221–1225.

Courchesne E, Ganz L, Norcia AM. Event-related potentials to human faces in infants. Child Development. 1981; 52:804–811. [PubMed: 7285651]

Darvas F, Ermer JJ, Mosher JC, Leahy RM. Generic head models for atlas-based EEG source analysis. Human Brain Mapping. 2006; 27:129–143. [PubMed: 16037984]

Darvas F, Schmitt U, Louis AK, Fuchs M, Knoll G, Buchner H. Spatiotemporal current density reconstruction (stCDR) from EEG/MET data. Brain Topography. 2001; 13:195–207. [PubMed: 11302398]

de Haan M, Johnson MH, Halit H. Development of face-sensitive event-related potentials during infancy: a review. International Journal of Psychophysiology. 2003; 51:45–58. [PubMed: 14629922]

de Haan M, Nelson CA. Recognition of the mother's face by six-month-old infants: A neurobehavioral study. Child Development. 1997; 68:187–210. [PubMed: 9179998]

de Haan M, Nelson CA. Brain activity differentiates face and object processing in 6-month-old infants. Developmental Psychology. 1999; 35:1113–1121. [PubMed: 10442879]

de Haan M, Pascalis O, Johnson MH. Specialization of neural mechanisms underlying face recognition in human infants. Journal of Cognitive Neuroscience. 2002; 14:199–209. [PubMed: 11970786]

Deffke I, Sander T, Heidenreich J, Sommer W, Curio G, Trahms L, Lueschow A. MEG/EEG sources of the N170-ms response to faces are co-localized in the fusiform gyrus. NeuroImage. 2007; 35:1495–1501. [PubMed: 17363282]

Delorme A, Makeig S. EEGLAB: an open source toolbox for analysis of single-trial EEG dynamics including independent component analysis. Journal of Neuroscience Methods. 2004; 134:9–21. [PubMed: 15102499]

Eimer M. Attentional modulations of event-related brain potentials sensitive to faces. Cognitive Neuropsychology. 2000; 17:103–116. [PubMed: 20945174]

Engell AD, Haxby JV. Facial expression and gaze-direction in human superior temporal sulcus. Neuropsychologia. 2007; 45:3234–3241. [PubMed: 17707444]

Fabiani, M.; Gratton, G.; Coles, MGH. Event-related brain potentials: Methods, theory, and applications. In: Cacioppo, JT.; Tassinary, LG.; Bernston, GG., editors. Handbook of psychophysiology. Cambridge University Press; New York: 2000. p. 53-84.

Ghazanfar AA, Chandrasekaran C, Logothetis NK. Interactions between the superior temporal sulcus and auditory cortex mediate dynamic face/voice integration in rhesus monkeys. The Journal of Neuroscience. 2008; 28:4469–4457.

Goren CC, Sarty M, Wu PYK. Visual following and pattern discrimination of face-like stimuli by newborn infants. Pediactrics. 1975; 56:544–549.

Guy MW, Reynolds GD, Zhang D. Visual attention to global and local stimulus properties in six-month-old infants: Individual differences and event-related potentials. Child Development. 2013; 84:1392–1406. [PubMed: 23379931]

Halit H, Csibra G, Volein Á, Johnson MH. Face-sensitive cortical processing in early infancy. Journal of Child Psychology and Psychiatry. 2004; 45:1228–1234. [PubMed: 15335343]

Halit H, de Haan M, Johnson MH. Cortical specialisation for face processing: Face-sensitive event-related potential components in 3- and 12-month-old infants. NeuroImage. 2003; 19:1180–1193. [PubMed: 12880843]

Hämäläinen JA, Ortiz-Mantilla S, Benaisch AA. Source localization of event-related potentials to pitch change mapped onto age-appropriate MRIs at 6 months of age. NeuroImage. 2011; 54:1910–1918. [PubMed: 20951812]

Iidaka T, Matsumoto A, Haneda K, Okada T, Sadato N. Hemodynamic and electrophysiological relationship involved in human face processing: Evidence from a combined fMRI-ERP study. Brain and Cognition. 2006; 60:176–186. [PubMed: 16387401]

Ishai A, Ungerleider LG, Martin A, Schouten JL, Haxby JV. Distributed representation of objects in the human ventral visual pathway. Proceedings of the National Academy of Sciences. 1999; 96:9379–9384.

Itier RJ, Taylor MJ. Source analysis of the N170 to faces and objects. Brain Imaging. 2004; 15:1261–1265.

Johnson MH, de Haan M, Oliver A, Smith W, Hatzakis H, Tucker LA, Csibra G. Recording and analyzing high-density event-related potentials with infants using the Geodesic sensor net. Developmental Neuropsychology. 2001; 19:295–323. [PubMed: 11758670]

Johnson MH, Dziurawiec S, Ellis H, Morton J. Newborns' preferential tracking of face-like stimuli and its subsequent decline. Cognition. 1991; 40:1–19. [PubMed: 1786670]

Johnson MH, Griffin R, Csibra G, Halit H, Farroni T, de Haan M, Richards J. The emergence of the social brain network: Evidence from typical and atypical development. Development and Psychopathology. 2005; 17:599–619. [PubMed: 16262984]

Kanwisher N, Damian S, Harris A. The fusiform face area is selective for faces not animals. NeuroReport. 1999; 10:183–187. [PubMed: 10094159]

Kanwisher N, McDermott J, Chun MM. The fusiform face area: A module in human extrastriate cortex specialized for face perception. The Journal of Neuroscience. 1997; 17:4302–4311. [PubMed: 9151747]

Kanwisher N, Yovel G. The fusiform face area: a cortical region specialized for the perception of faces. Philosophical Transactions of The Royal Society B. 2006; 361:2109–2128.

Key APF, Stone WL. Processing of novel and familiar faces in infants at average and high risk for autism. Developmental Cognitive Neuroscience. 2012; 2:244–255. [PubMed: 22483074]

Key APF, Stone W, Williams SM. What do infants see in faces? ERP evidence of different roles of eyes and mouth for face perception in 9-month-olds. Infant and Child Development. 2009; 18:149–162. [PubMed: 26052254]

Kouider S, Stahlhut C, Gelskov SV, Barbosa LS, Dutat M, de Gardelle V, Dehaene-Lambertz G. A neural marker of perceptual consciousness in infants. Science. 2013; 340:376–380. [PubMed: 23599498]

Leppänen JM, Moulson MC, Vogel-Farley VK, Nelson CA. An ERP study of emotional face processing in the adult and infant brain. Child Development. 2007; 78:232–245. [PubMed: 17328702]

Lopez-Calderon J, Luck SJ. ERPLAB: an open-source toolbox for the analysis of event-related potentials. Frontiers in Human Neuroscience. 2014; 8 doi: 10.3389/fnhum.2014.00213.

Macchi Cassia V, Kuefner D, Westerlund A, Nelson CA. A behavioural and ERP investigation of 3-month-olds' face preferences. Neuropsychologia. 2006; 44:2113–2125. [PubMed: 16368116]

Macchi Cassia V, Turati C, Simion F. Can a nonspecific bias toward top-heavy patterns explain newborns' face preference? Psychological Science. 2004; 15:379–383. [PubMed: 15147490]

Mallin BM, Richards JE. Peripheral stimulus localization by infants of moving stimuli on complex backgrounds. Infancy. 2012; 17:692–714. [PubMed: 24672284]

McCleery JP, Akshoomoff N, Dobkins KR, Carver LJ. Atypical face versus object processing and hemispheric asymmetries in 10-month-old infants at risk for autism. Biological Psychiatry. 2009; 66:950–957. [PubMed: 19765688]

McCleery, JP.; Richards, JE. Comparing realistic head models for cortical source localization of infant event-related potentials; Poster presented at the International Conference on Infant Studies; Minneapolis, MN. Jun. 2012 2012

Morton J, Johnson MH. CONSPEC and CONLERN: A two-process theory of infant face recognition. Psychological Review. 1991; 95:164–181. [PubMed: 2047512]

Nasr S, Tootell RBH. Role of fusiform and anterior temporal cortical areas in facial recognition. NeuroImage. 2012; 63:1743–1753. [PubMed: 23034518]

Ortiz-Mantilla S, Hämäläinen JA, Benaisch AA. Time course of ERP generators to syllables in infants: A source localization study using age-appropriate brain templates. NeuroImage. 2012; 59:3275–3287. [PubMed: 22155379]

Pascalis O, de Schonen S, Morton J, Deruelle C, Fabre-Grenet M. Mother's face recognition by neonates: A replication and an extension. Infant Behavior and Development. 1995; 18:79–85.

Pascual-Marqui RD. Standardized low-resolution brain electromagnetic tomography (sLORETA): technical details. Methods and Findings in Experimental and Clinical Pharmacoogy. 2002; 24:5–12.

Pascual-Marqui RD, Michel CM, Lehmann D. Low-resolution electromagnetic tomography - A new method for localizing electrical activity in the brain. International Journal of Psychophysiology. 1994; 18:49–65. [PubMed: 7876038]

Pempek TA, Kirkorian HL, Richards JE, Anderson DR, Lund AF, Stevens M. Video comprehensibility and attention in very young children. Developmental Psychology. 2010; 46:1283–1293. [PubMed: 20822238]

Peykarjou S, Pauen S, Hoehl S. How do 9-month-old infants categorize human and ape faces? A rapid repetition ERP study. Psychophysiology. 2014; 51:866–878. [PubMed: 24890394]

Picton TW, Bentin S, Berg P, Donchin E, Hillyard SA, Johnson R, Taylor MJ. Guidelines for using human event-related potentials to study cognition: Recording standards and publications criteria. Psychophysiology. 2000; 37:127–152. [PubMed: 10731765]

Pitcher D, Walsh V, Duchaine B. The role of the occipital face area in the cortical face perception network. Experimental Brain Research. 2011; 209:481–493. [PubMed: 21318346]

Reynolds GD, Courage ML, Richards JE. Infant attention and visual preferences: Converging evidence from behavior, event-related potentials, and cortical source localization. Developmental Psychology. 2010; 46:886–904. [PubMed: 20604609]

Reynolds GD, Richards JE. Cortical source localization of infant cognition. Developmental Neuropsychology. 2009; 34:312–329. [PubMed: 19437206]

Richards JE. Attention affects the recognition of briefly presented visual stimuli in infants: an ERP study. Developmental Science. 2003; 6:312–328. [PubMed: 16718304]

Richards JE. Localizing cortical sources of event-related potentials in infants' covert orienting. Developmental Science. 2005; 8:255–278. [PubMed: 15819757]

Richards JE. Cortical sources of ERP in prosaccade and antisaccade eye movements using realistic source models. Frontiers in Systems Neuroscience. 2013:7. doi: 10.3389/fnsys.2013.00027. [PubMed: 23596400]

Richards JE, Boswell C, Stevens M, Vendemia JMC. Evaluating methods for constructing average high-density electrode positions. Brain Topography. 2015a; 28:70–86. [PubMed: 25234713]

Richards JE, Sanchez C, Phillips-Meek M, Xie W. A database of age-appropriate average MRI templates. NeuroImage. 2015b doi: 10.1016/j.neuroimage.2015.04.055.

Richards, JE.; Xie, W. Brains for all the ages: Structural neurodevelopment in infants and children from a life-span perspective. In: Benson, J., editor. Advances in Child Development and Behavior. Vol. 48. Elsevier; Philadephia, PA: 2015. p. 1-52.chapter 1DOI:10.1016/bs.acdb.2014.11.001

Rossion B, Gauthier I, Tarr MJ, Despland P, Bruyer R, Linotte S, Crommelinck M. The N170 occipito-temporal component is delayed and enhanced to inverted faces but not to inverted objects: an electrophysiological account of face-specific processes in the human brain. NeuroReport. 2000; 11:69–74. [PubMed: 10683832]

Rossion B, Hanseeuw B, Dricot L. Defining face perception areas in the human brain: A large-scale factorial fMRI face localizer analysis. Brain and Cognition. 2012; 79:138–157. [PubMed: 22330606]

Rossion B, Joyce CA, Cottrell GW, Tarr MJ. Early lateralization and orientation tuning for face, word, and object processing in the visual cortex. NeuroImage. 2003; 20:1609–1624. [PubMed: 14642472]

Sadeh B, Podlipsky I, Zhdanov A, Yovel G. Event-related potential and functional MRI measures of face selectivity are highly correlated: A simultaneous ERP-fMRI investigation. Human Brain Mapping. 2010 doi: 10.1002/hbm.20952.

Scott LS, Monesson A. Experience-dependent neural specialization during infancy. Neuropsychologia. 2010; 48:1857–1861. [PubMed: 20153343]

Scott LS, Shannon RW, Nelson CA. Neural correlates of human and monkey face processing in 9-month-old infants. Infancy. 2006; 10:171–186.

Searle, SR. Linear models for unbalanced data. Wiley; New York: 1987.

Shibata T, Nishijo H, Tamura R, Miyamoto K, Eifuku S, Endo S, Ono T. Generators of visual evoked potentials for faces and eyes in the human brain as determined by dipole localization. Brain Topography. 2002; 15:51–63. [PubMed: 12371677]

Tucker DM. Spatial sampling of head electrical fields - the Geodesic Sensor Net. Electroencephalography and Clinical Neurophysiology. 1993; 87:154–163. [PubMed: 7691542]

Vatta F, Meneghini F, Esposito F, Mininel S, Di Salle F. Realistic and spherical head modeling for EEG forward problem solution: A comparative cortex-based analysis. Computational Intelligence and Neuroscience. 20102010 doi: 10.1155/2010/972060.

Webb SJ, Long JD, Nelson CA. A longitudinal investigation of visual event-related potentials in the first year of life. Developmental Science. 2005; 8:605–616. [PubMed: 16246251]

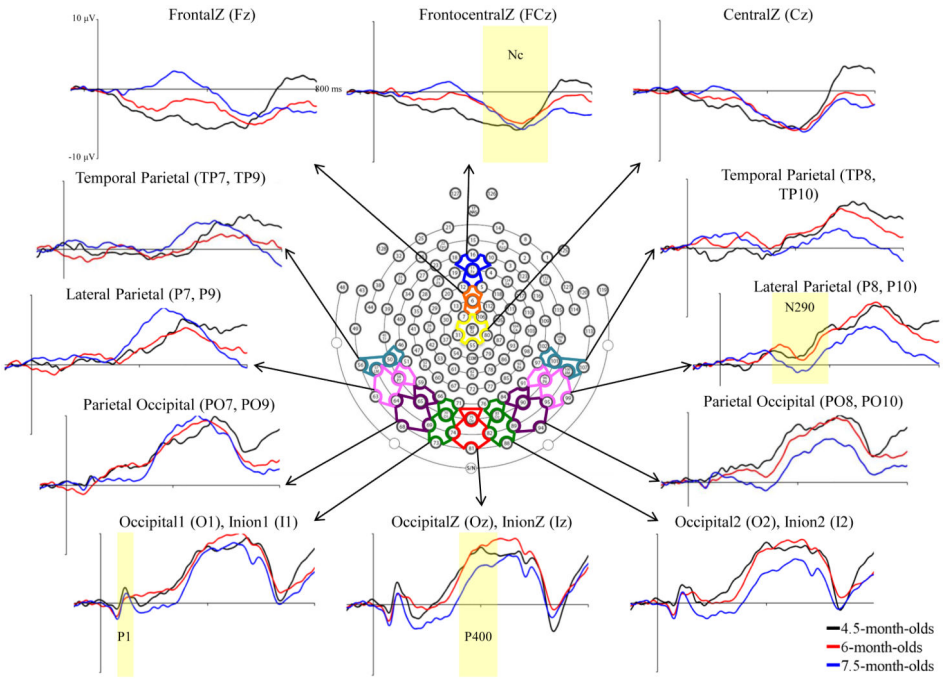

Figure 1.

Grand average ERP activity across GSN Electrodes and virtual 10-10 electrode clusters. The ERP changes are shown from 50 ms preceding stimulus onset through 800 ms post-stimulus, separately for the three testing ages.

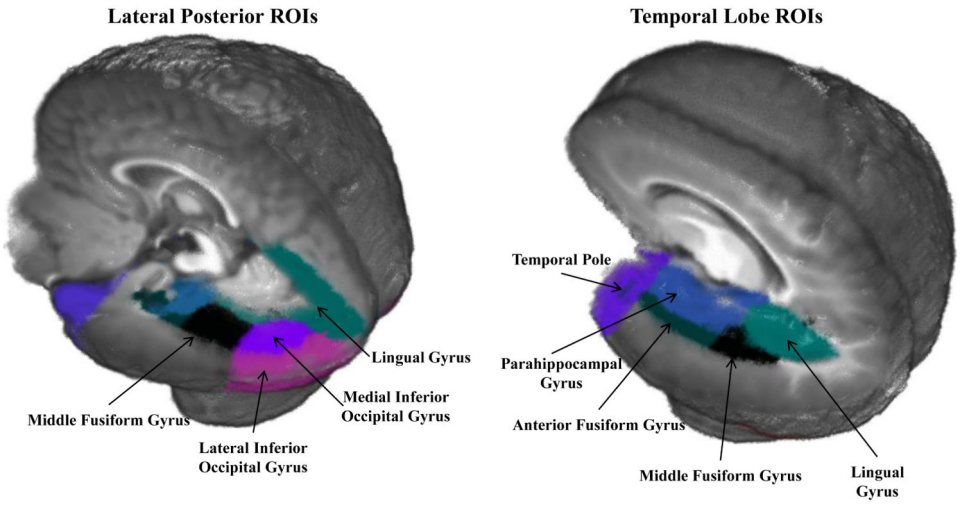

Figure 2.

Regions of interests (ROIs) shown on the 6-month-old average age-appropriate template. These regions are the most relevant theoretically for the processing of faces.

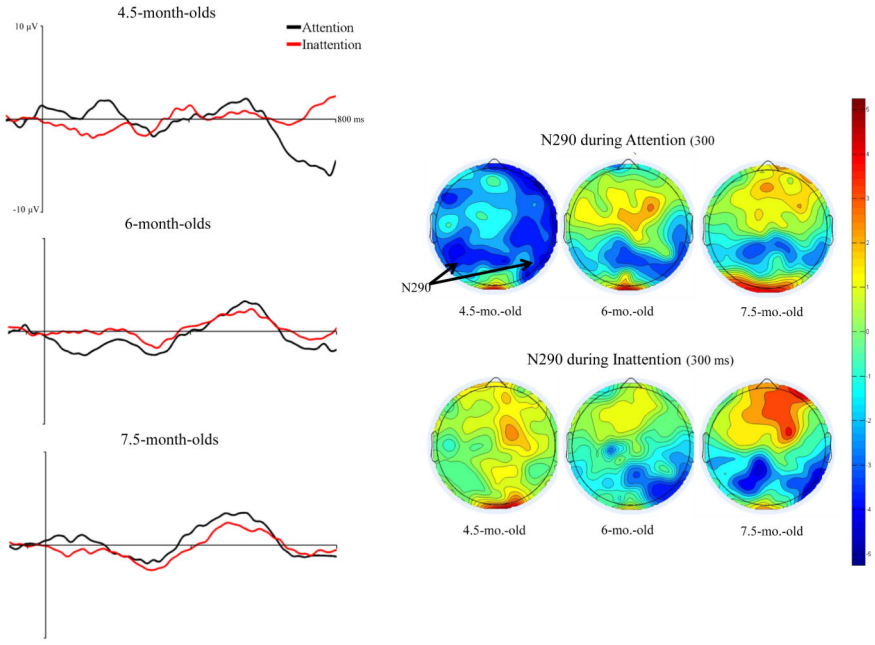

Figure 3.

The effect of HR-defined periods of attention on the N290 ERP response. The left panels show the ERP from 50 ms preceding stimulus through 800 ms following stimulus onset averaged over lateral posterior-inferior scalp areas (PO7-10, P7-10, and TP7-10). The figures have separate lines for the HR-defined periods of attention and inattention, graphed separately for the three testing ages. The right panels show scalp topographical potential maps at the peak latency for the N290 for faces and toys during attention, separately for the three testing ages.

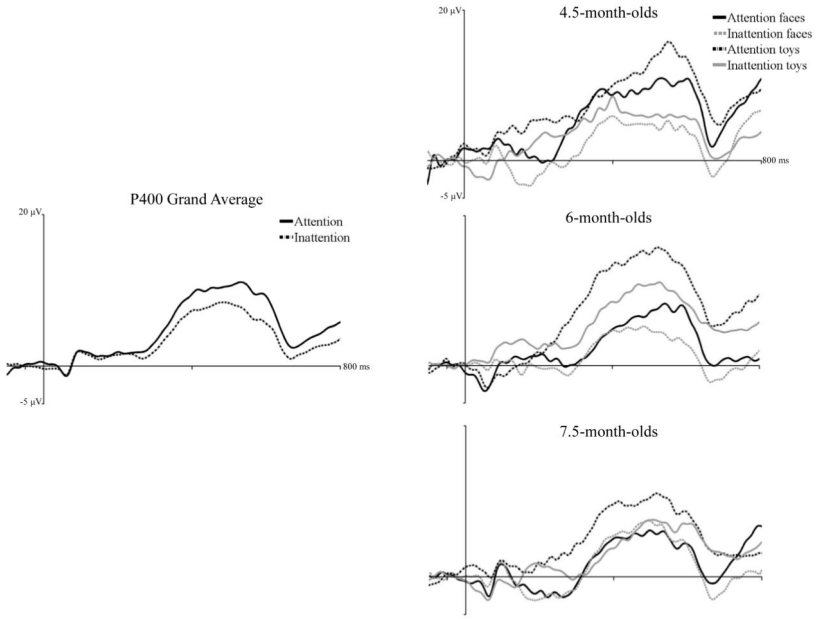

Figure 4.

The effect of attention on P400 responses to faces and toys. The panels show the ERP response from 50 ms preceding stimulus onset through 800 ms following stimulus onset averaged over medial posterior-inferior scalp areas (PO7-10, O1-2, I1-2, Oz, and Iz). The left panel shows the response averaged over all ages, separately for HR-defined periods of attention and inattention. The right panels show the responses separately for responses during attention to faces, attention to toys, inattention to faces, and inattention to toys, done separately for the three testing ages.

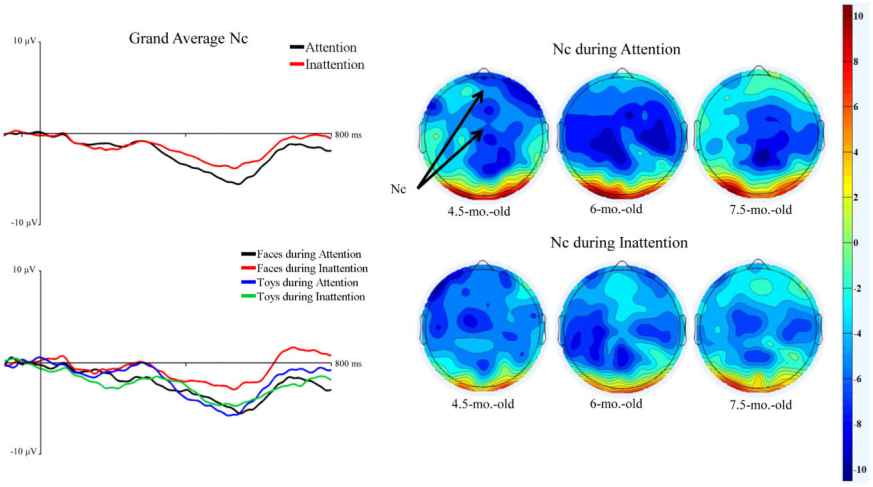

Figure 5.

The effect of HR-defined periods of attention on Nc responses to faces and toys. The left panels show the ERP from 50 ms preceding stimulus through 800 ms following stimulus onset averaged over frontal and central midline virtual electrodes (Fz, FCz, and Cz). The graphs are shown averaged over all the ages but separately for attention and inattention (left panels, top figure) and separately for responses during attention to faces, attention to toys, inattention to faces, and inattention to toys (left panels, bottom figure). The right panels show scalp topographical maps for at the Nc latency (400 – 600 ms) separately for attention and toys, and separately for the three testing ages.

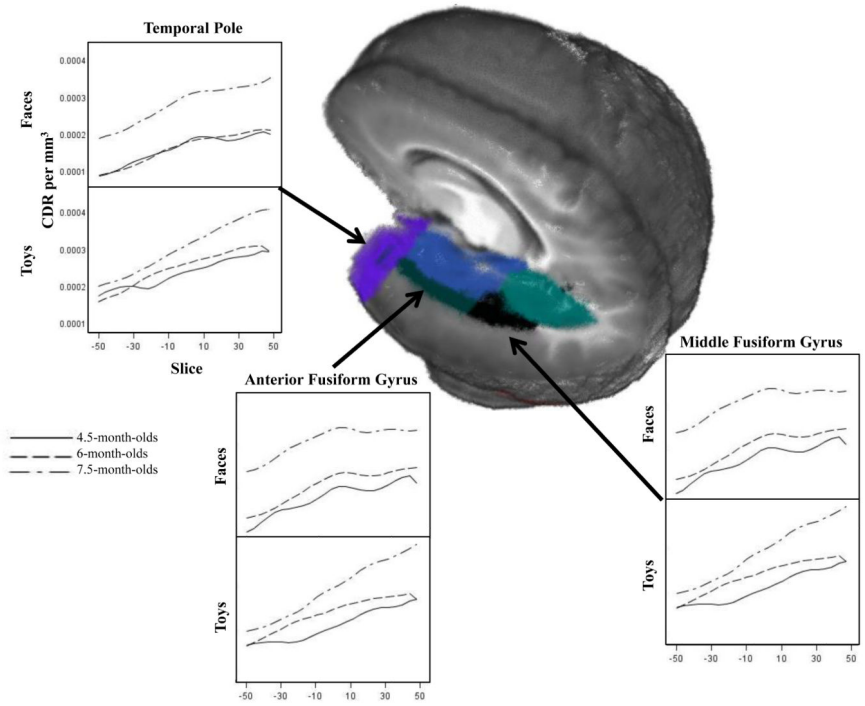

Figure 6.

CDR amplitude at temporal lobe ROIs during the time period of the N290 in response to faces and toys. The panels show the CDR amplitude from −50 ms to +50 ms centered at the peak latency of the N290 for three temporal lobe ROIs that showed age and attention effects. The panels show the responses separately for the three testing ages, separated by the response to faces and toys.

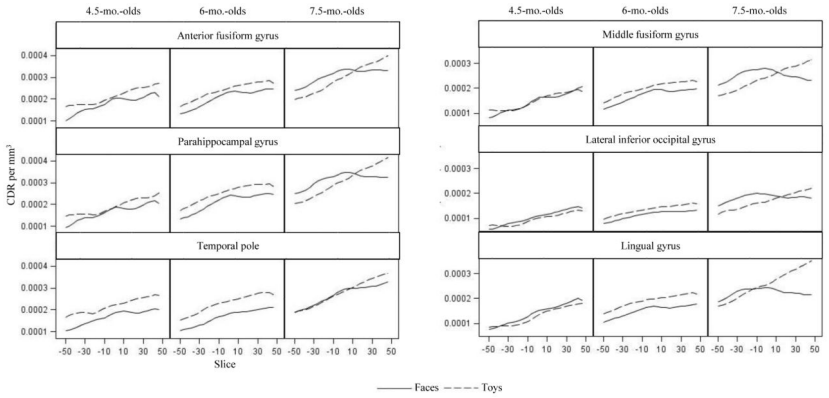

Figure 7.

N290 current density across ROIs. The panels show the CDR amplitude from −50 ms to +50 ms centered at the peak latency of the N290, separately for faces and toys, and separate for the three testing ages. These ROIs shows significant activation in the time period of the N290 latency.

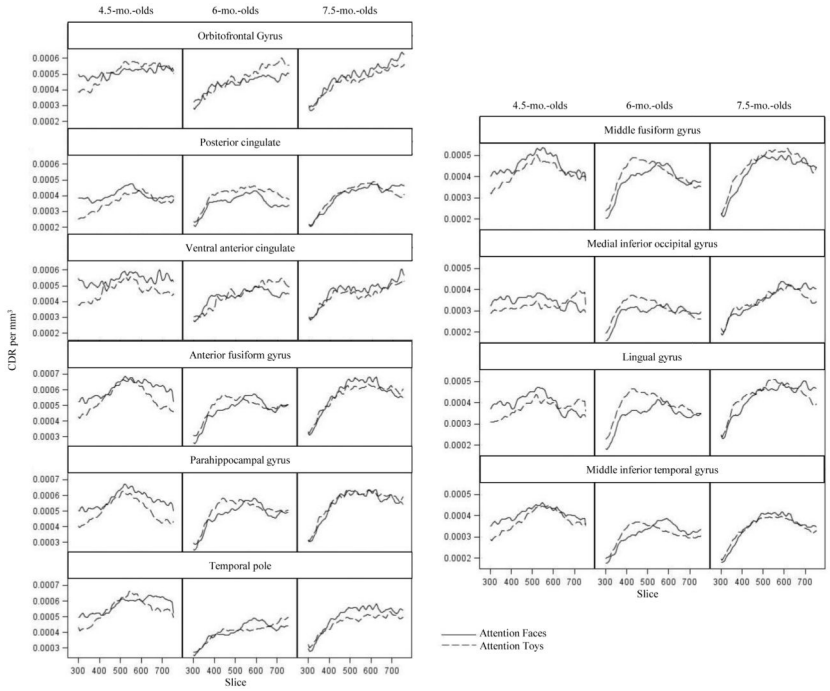

Figure 8.

P400/Nc current density across ROIs. The panels show the CDR amplitude from 300 to 750 ms following stimulus onset, separately for attention to faces and attention to toys, and separate for the three testing ages. These ROIs shows significant activation in the time period between 400-600 ms. across midline frontal and parietal ROIs, anterior temporal ROIs, and posterior temporal and occipital ROIs.